Design, Performance and Cabling Analysis of Nb_3Sn Wires for the FCC Study

Simon C Hopkins, Algirdas Baskys, Bernardo Bordini, Jerome Fleiter and Amalia Ballarino

Technology Department, European Organization for Nuclear Research (CERN), 1211 Geneva 23, Switzerland

E-mail: simon.hopkins@cern.ch

Abstract. The hadron collider proposed by the Future Circular Collider (FCC) study would require high-field superconducting magnets capable of producing a dipole field of around 16 T in a 50 mm aperture. To develop a suitable conductor for these magnets, CERN is coordinating a conductor development programme aiming to obtain Nb_3Sn wire with a non-copper critical current density of 1500 A mm^{-2} at 16 T and 4.2 K, in lengths suitable for manufacturing 14 m long magnets, and able to withstand cabling without significant degradation. Here we report the superconducting characterisation and quantitative microscopy of recently-developed Nb_3Sn wires with novel layouts and compositions, and evaluate their suitability for Rutherford cabling based on cabling trials and rolling studies. An analysis of the influence of wire layout, materials and mechanical characteristics on cabling performance is presented, to support recommendations for future wire designs.

1. Introduction

In parallel with CERN's High-Luminosity LHC (HL-LHC) Project, a major upgrade programme to increase the luminosity of the Large Hadron Collider (LHC) that is entering the construction phase, the Future Circular Collider (FCC) Study has been developing conceptual designs for its potential successor [1].

The proposed future hadron collider, either a 100 TeV centre-of-mass energy machine in a new 100 km tunnel (FCC-hh) [2] or an energy upgrade of the LHC (HE-LHC), would require main dipole magnets with an operating field of 16 T (at 1.9 K) and a magnetic length of ~14 m; and a conductor development programme [3] has been established to develop suitable Nb_3Sn wire, in collaboration with academic and industrial partners. In addition to achieving cost and performance targets [3] including a non-copper critical current density (J_c) of 1500 A mm^{-2} at 16 T and 4.2 K, the programme aims to demonstrate that the wires under development can be manufactured in sufficiently long piece lengths to allow the efficient manufacture of magnets at the required scale, and that they can withstand Rutherford cabling without significant degradation.

An interim target corresponding to the J_c specified for HL-LHC, extrapolating to ~1000 A/mm^2 at 16 T and 4.2 K, has been achieved for the first time by three participating manufacturers [3] in reasonably long unit lengths. In particular, TVEL (Russia) has supplied 12 km of wire in unit lengths averaging over 1 km; JASTEC has supplied ~1 km, while focusing on trials of different wire designs;

and very recently KAT has produced 6 km of wire with an average unit length of 220 m. It is therefore timely to assess the suitability of these wires for cabling.

The specification for HL-LHC cables produced from internal tin Nb_3Sn wires requires extracted strands to have a residual resistance ratio (RRR) exceeding 100, with a critical current (I_c) degradation not exceeding 5 % relative to the virgin (as-received) wire; and similar requirements apply to wire samples rolled with a reduction of 15 %.

In this article, uniaxial rolling tests and the preparation of a 40-strand Rutherford cable are reported for selected wires from the FCC conductor development programme. I_c and RRR measurements of rolled wires and strands extracted from cables are assessed against the HL-LHC specification, and micrographs of the wire cross-sections after rolling and cabling are presented and quantitatively analysed.

2. Methods

Superconducting characterisation, microscopy and image analysis were performed on as-received wire, wires after rolling, and strands extracted from Rutherford cables.

2.1. Rolling and Cabling Methods

Rolled samples were prepared using a manually-operated uniaxial rolling mill.

Rutherford cabling was performed using a planetary cabling machine equipped with 40 spools with independent tension monitoring and control, with on-line measurement of the cable thickness and continuous imaging and analysis of the cable surface and edge facets [4].

The cable layout used for these trials is a 40-strand design with a stainless steel core 14 mm wide and 25 μm thick, developed for the ERMC coil of the FCC magnet development programme based on the design previously used for FRESCA 2 [5]. The cable has a width of 20.85 mm, a thickness of 1.82 mm, a transposition pitch of 100 mm and no keystone angle. After production, strands were extracted for measurement from the leading end of the cable.

2.2. Superconducting Characterisation

The following samples were prepared from unreacted wire: for critical current (I_c) measurement, a ~1.2 m length wound on a coated Ti–6Al–4V VAMAS-type barrel; for residual resistivity ratio (RRR), a straight length of ~150 mm; and for magnetization measurements, either a straight sample ~6 mm in length, or a mini-coil wound on a 5 mm thread to obtain a total length of ~125 mm. The manufacturer's recommended heat treatment was then performed under vacuum on this set of samples.

Transport critical current (I_c) measurements were performed in liquid helium (4.3 K) at 12–15 T, with a voltage tap spacing of 60 cm, and applying an electric field criterion of 0.1 μV/cm. Fitting and extrapolation of $I_c(B)$ data used the procedure in [6], with pinning force parameters $p = 0.5$ and $q = 2$. Magnetization was measured using a vibrating sample magnetometer (VSM; Cryogenic, UK) at 4.2 K with a field range of ± 10 T, from which the effective filament diameter (d_{eff}) was determined by comparison with the scaled transport J_e [4]. RRR was calculated from four-point resistance measurements at room temperature and ~20 K.

2.3. Microscopy and Image Analysis

The majority of wire samples for microscopy were cut, supported in a brass holder and hot mounted in a conductive phenolic resin. In some cases for which only optical microscopy was planned, cold mounting was used. The mounted specimens were prepared for examination with a sequence of grinding (SiC paper) and polishing (diamond suspension) steps down to 1 μm or smaller.

Scanning electron microscopy (SEM) was performed using a Zeiss Sigma field emission SEM, typically using an accelerating voltage of 10 kV, and energy-dispersive x-ray spectroscopy (EDX) was used for compositional analysis.

In order to obtain high resolution images over large areas for analysis, in many cases multiple images were stitched using an automated algorithm. Image analysis was performed using scripts

written in Python, making use of the NumPy and SciPy libraries and toolkits. Images were segmented using a *k*-means clustering algorithm, and the resulting binary (monochrome) images for each component were used for further geometrical analysis (see [7]).

3. Wire Designs

Two wires developed by industrial partners in the FCC conductor development programme were selected for evaluation of their suitability for cabling, on the basis that they had achieved a non-Cu J_c performance at 4.2 K of at least 1000 A/mm^2 at 16 T and 2500 A/mm^2 at 12 T, exceeding the HL-LHC specification, in sufficiently long lengths for cabling to be feasible. They also represent significantly different approaches to internal tin wire design: distributed barrier for TVEL, and common-barrier distributed tin for JASTEC.

The wire from TVEL, a 37 sub-element design with distributed niobium barriers, was developed by the Bochvar Institute (VNIINM) and produced at Chepetsky Mechanical Plant (ChMP) at the end of 2017 [8]. 12 km of wire was supplied in piece lengths averaging more than 1 km; for comparison, the minimum piece length accepted for HL-LHC wire procurement was 720 m.

In the context of a joint collaborative programme between CERN and the Energy Accelerator Research Organization, KEK (Japan), JASTEC has been producing a series of trial wires with a distributed tin design [9]. The general design consists of a single common Nb barrier, with Ti-doped Sn distributed in islands between multifilamentary Nb modules. The wire reported here is from the third trial, in which a significantly reduced sub-element size was achieved in 0.8 mm diameter wires [3]. Tests have been performed on two similar variants, referred to as ‘trial 3: 1’ and ‘trial 3: 2’.

Key characteristics of the wires are summarised in Table 1; further details [3] and analysis [7] have been previously reported.

Table 1. Key characteristics of the selected wires

Parameter	TVEL	JASTEC
Wire diameter (mm)	1.0	0.8
Cu/non-Cu ratio	1.2 ± 0.2	1.0 ± 0.2
Diffusion barriers	Distributed Nb barriers	Common Nb barrier
Number of sub-elements	37	139 Nb, 72 Sn-Ti
Geometrical sub-element diameter (μm)	107 – 112	
Effective filament diameter, d_{eff} (μm)[a]	132 – 144	55
Maximum non-Cu J_c, 16 T 4.2 K (A/mm^2)[b]	1140	1090

[a] Evaluated on 6 mm straight samples
[b] Extrapolated from measurements as 12 – 15 T

4. Rolling Behaviour of the JASTEC Distributed Tin Wire

4.1. Superconducting Performance after 15 % Rolling Reduction

Critical current measurements at CERN revealed no degradation of the I_c of the JASTEC wire after rolling with a 15 % reduction: indeed, a small increase (~4 %) was found for the present samples (Figure 1), but the reproducibility and exact cause of this increase has not yet been determined. Although the very high (~400) RRR of the as-received wire is approximately halved after rolling, it remains very much higher than the specification of 100 for rolled samples, suggesting that the external diffusion barrier remains intact.

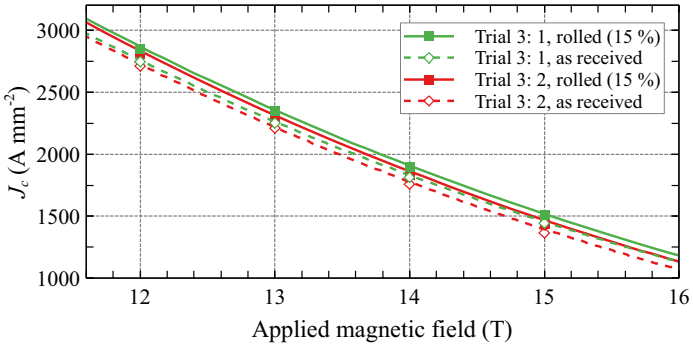

Figure 1: Non-copper J_c of two variants of JASTEC's third trial wire, as received and after rolling with a 15 % reduction. In all cases, results are averaged from two samples.

Table 2. RRR of two samples each of the two variants of JASTEC's third trial wire, in the as-received (round) condition and after rolling with 15 % reduction

Parameter	Trial 3: 1		Trial 3: 2	
	Sample 1	Sample 2	Sample 1	Sample 2
Round	398	400	358	351
Rolled (15 % reduction)	213	194	179	171

4.2. Image Analysis after 15 % Rolling Reduction

Four samples of each wire variant were examined by SEM: two of each in the as-received condition, and two after rolling with a 15 % reduction. An example of the overall wire cross-section after reaction is presented in Figure 2. All samples demonstrated similar deformation behaviour, so they will be considered together in the following analysis.

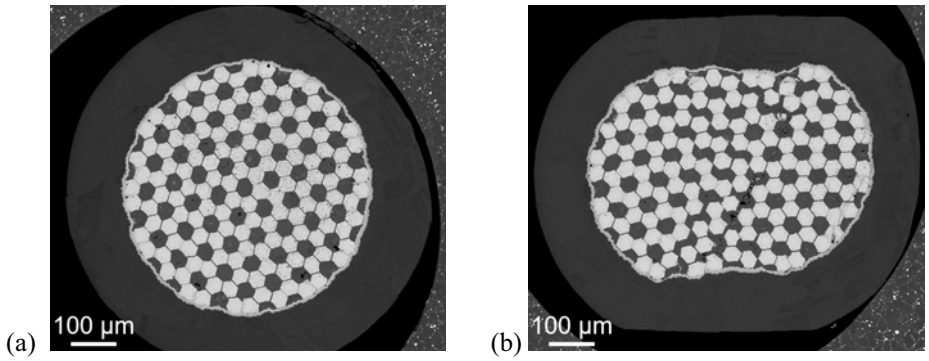

Figure 2: SEM micrographs of the cross-section of a JASTEC sample (from trial 3: 1), (a) as received and (b) after 15 % rolling, after heat treatment (backscattered electron image, 10 kV).

To assess the nature of the deformation, image analysis was performed: in particular, the aspect ratio of the sub-elements was quantified in round and rolled samples, and the separation of the sub-elements from their neighbours was evaluated.

For typical internal tin conductors, the distribution of aspect ratios is expected to broaden after strong deformation in rolling or cabling [10]. As shown in Figure 3(a), the distribution of aspect ratios changes very little on rolling with a 15 % reduction, suggesting that the deformation of the wire was accommodated primarily by displacement of the sub-elements (with shearing in the copper matrix)

rather than distortion of the sub-elements (corresponding to relative displacement or shearing of the niobium filaments).

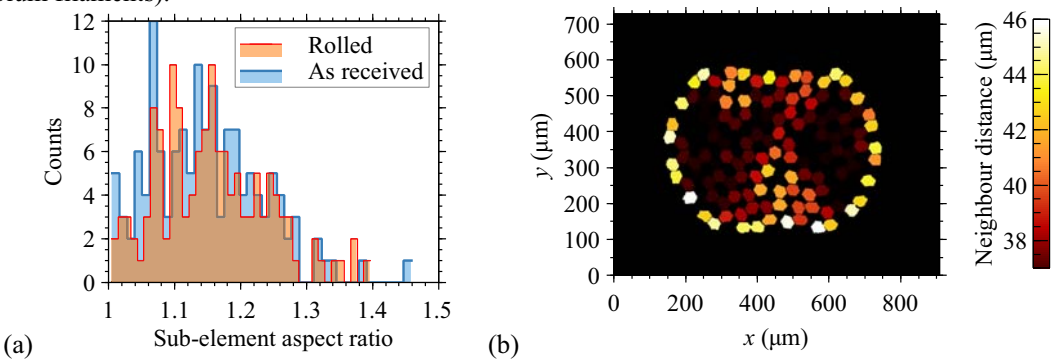

Figure 3: Results of SEM image analysis for a JASTEC wire (trial 3: 1) after reaction: (a) the sub-element aspect ratio distribution for as-received (round) and rolled (15 % reduction) samples, and (b) a map of the variation in the average distance to the three nearest neighbour sub-elements, with a colour scale emphasising those with a separation of more than 37 μm.

Figure 3(b) shows, with a colour scale, the average distance from each sub-element to its nearest three neighbours; the scale is defined such that closely-spaced sub-elements appear dark. This confirms that the relative displacement of sub-elements is highest near the centre and along the diagonals, where shear bands are expected to form. The high nearest-neighbour distance for peripheral sub-elements is due to there only being two immediate neighbours in these sites.

Examining an enlargement of this most distorted region (Figure 4), the planes on which shearing has occurred in the copper matrix are apparent. There are very few instances of significant sub-element distortion, as expected from the aspect ratio analysis: this is beneficial for enabling complete and uniform reaction, e.g. by maintaining the copper channels through which tin diffuses, and is consistent with the absence of I_c degradation on rolling for this wire design.

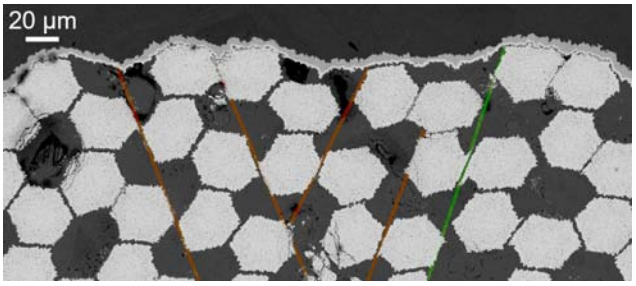

Figure 4: Higher magnification SEM micrograph of a 15 % rolled JASTEC sample (trial 3: 1) after reaction, indicating the paths along which shearing has occurred: primarily confined to copper channels (red), and in one case with some sub-element distortion (green, right-most).

Another consequence of rolling is that the Nb diffusion barrier has thinned. In combination with the partial reaction to Nb_3Sn of this barrier that occurs (both in the round and rolled wires), and the imperfect uniformity of the original barrier thickness, this results in an increased risk of tin leak into the stabilising copper. This is evidenced by the extending tail towards zero thickness of the barrier thickness distribution in the rolled wire (Figure 5). The RRR measurements suggest that little or no tin leak occurred in the samples tested, but localised instances of near-zero unreacted barrier thickness in

the metallographic samples indicate that optimisation of the barrier uniformity and thickness may be required for reliable long-length cabling. A similar observation was made previously for distributed tin wires from KAT [7], and is a characteristic likely to require particular attention for all common-barrier distributed tin wires.

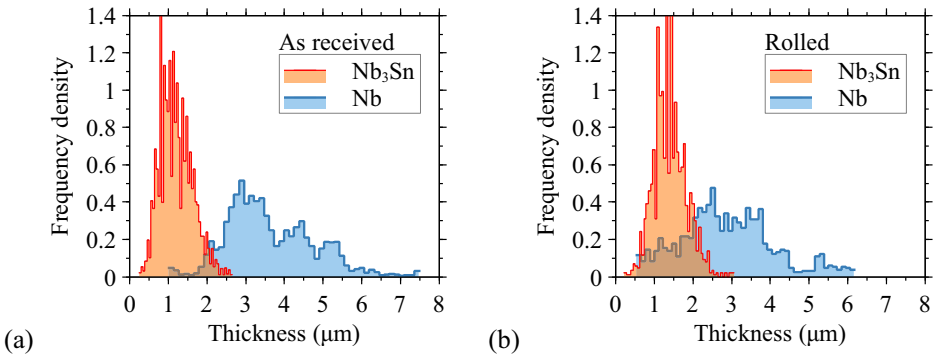

Figure 5: Thickness distribution of the unreacted (Nb) and reacted (Nb_3Sn) portions of the diffusion barrier in the JASTEC wire after reaction, for (a) a round and (b) a rolled sample. The analysis was performed for a sample of the barrier region, not the full length.

4.3. Dependence on Rolling Reduction

The nominal thickness reduction on cabling would correspond to approximately a 10 % rolling reduction; but in practice a strand experiences less regular conditions during cabling, with more severe deformation occurring periodically along the cable length (see section 5). To assess the sensitivity of the deformation behaviour to the rolling reduction, optical microscopy was performed for samples at reductions between 5 % and 30 % (Figure 6).

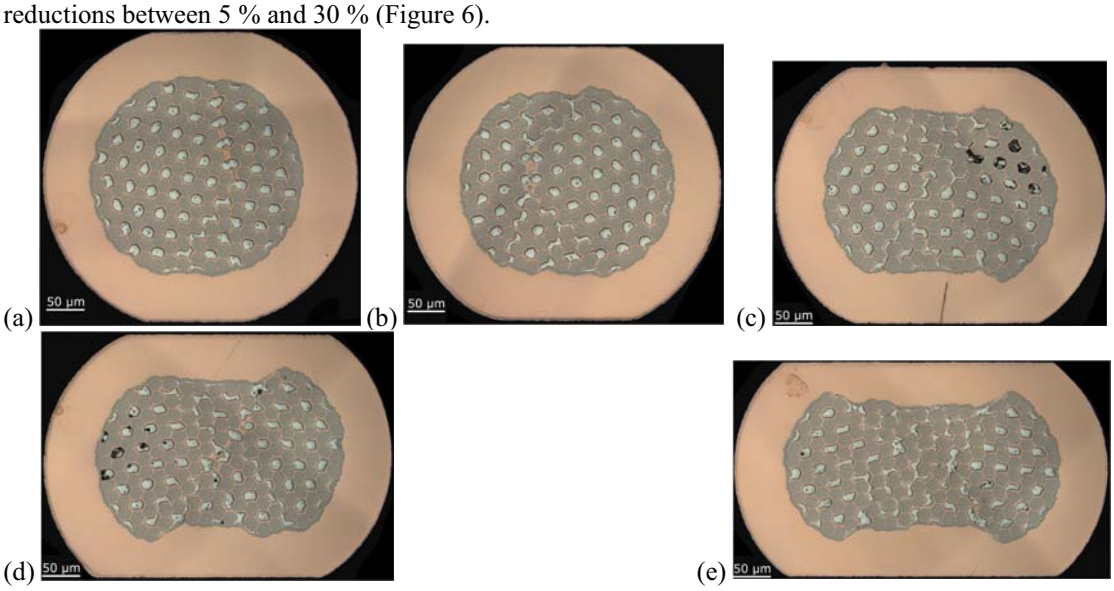

Figure 6: Optical micrographs of the JASTEC wire (trial 3: 1) after rolling reductions of (a) 5 %, (b) 10 %, (c) 15 %, (d) 20 % and (e) 30 %.

The onset of shear deformation, primarily confined to the copper matrix and soft tin regions along the diagonals, is evident even for a rolling reduction of 5 %. The voids that appear to open at 10 % reduction, away from the typical axis of peak shear strain, result in less symmetric deformation, and

may imply locally imperfect adhesion between modules. This may require further study, particularly in the less regular deformation environment of a Rutherford cable. As the rolling reduction increases, increasingly more bands are engaged in the region between the diagonals, as discussed in section 4.2, and the relative displacement and rotation between adjacent, relatively undistorted clusters of niobium sub-elements grows.

These unreacted wire cross-sections demonstrate the substantial distortion of the tin regions, which increasingly coalesce as the reduction increases. The increasingly non-uniform tin supply is likely to cause locally incomplete reaction, and hence I_c degradation, at large reductions. The increasing distortion and thinning of the diffusion barrier is also apparent, with breaches in the diagonal positions becoming apparent at 20 % reduction. The resulting tin leak is likely to cause RRR degradation and contribute to I_c degradation, so these defects imply a limit to the acceptable rolling reduction of between 15 % and 20 %.

Tests by JASTEC, up to a rolling reduction of 20 %, have shown similar results: clear barrier breaches were not identified after 20 % reduction, but a non-Cu J_c degradation of 7 % was measured, compared to 0 % for a 15 % reduction.

5. Cabling of the TVEL Distributed Barrier Wire

5.1. Microscopy of Rolled Wire

The cross-section of the TVEL wire, as received and after a 15 % rolling reduction, is shown in Figure 7. A prominent feature of this wire, even as received, is the geometrical distortion of peripheral sub-elements: it has been shown previously that this results in incomplete reaction of the sub-element 'tips' [7]. The imperfect symmetry of the round wire contributes to non-uniformity of the cross-section after rolling, and increasingly irregular sub-element shapes are likely to influence the extent of Nb_3Sn formation. However, in the examples examined, the sub-element diffusion barriers remained intact.

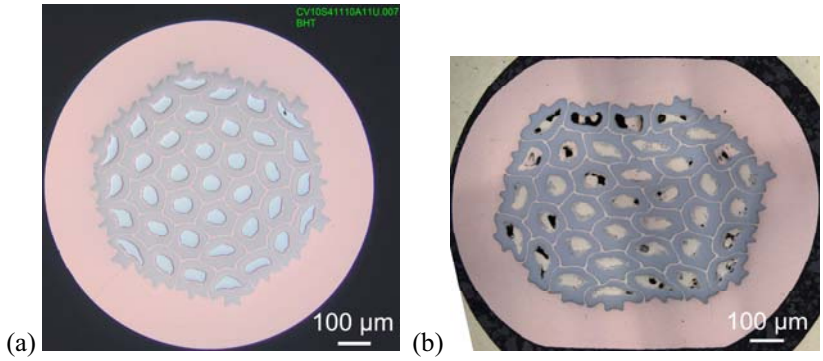

Figure 7: Optical micrographs of samples of the TVEL wire: (a) as received, unreacted and (b) after rolling with a 15 % reduction, reacted.

5.2. Cable Production and Microscopy

A trial length of 55 m of Rutherford cable was produced using strands from four unit lengths of the TVEL wire, originating from two different billets.

Two examples of the cross-section of the resulting cable are shown in Figure 8. These examples are close to the two limiting cases for the edge configuration, with the outermost strands centred on the same plane as their neighbours or on the mid-plane of the cable respectively.

It is clear from Figure 8(a) that particularly strong distortion of the overall strand cross-section can occur for strands located near the cable edges, depending on the exact strand configuration. This strong and non-uniform deformation can result in severe distortion of the sub-element geometry, as

presented in Figure 8(b) and (c): shearing of sub-elements can result in a local breach in the diffusion barrier and/or merging of the tin cores of adjacent sub-elements.

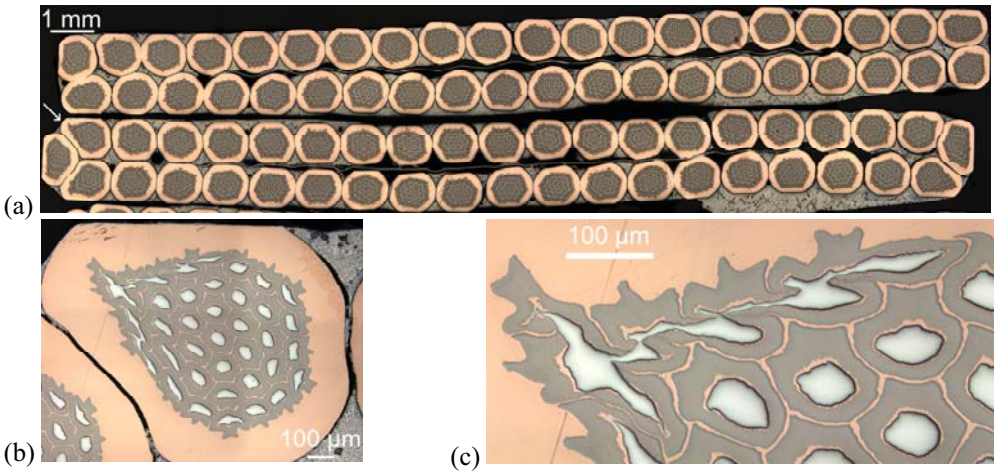

Figure 8: Optical micrographs of the cross-section of the TVEL cable: (a) two examples of the full cross-section, (b) the significantly deformed strand marked with an arrow in the cable cross-section, and (c) an enlargement of the strand showing a selection of damaged sub-elements.

By analysing a sample of 5 cable cross-sections, these damaged sub-elements have been enumerated as a function of strand position in the cable cross-section (Figure 9). As might be expected from the analysis of the rolled sample, none of these defects arise for most strand positions. However, ~5 per strand are commonly found for strands at the cable edges in the configuration with the most severe deformation (sometimes called the 'triplet' configuration [11]), corresponding to the kink in the outermost strand as it traverses between the layers, as in the case of Figure 8(b). It should be noted that all strands will periodically experience these deformation conditions along the length of the cable.

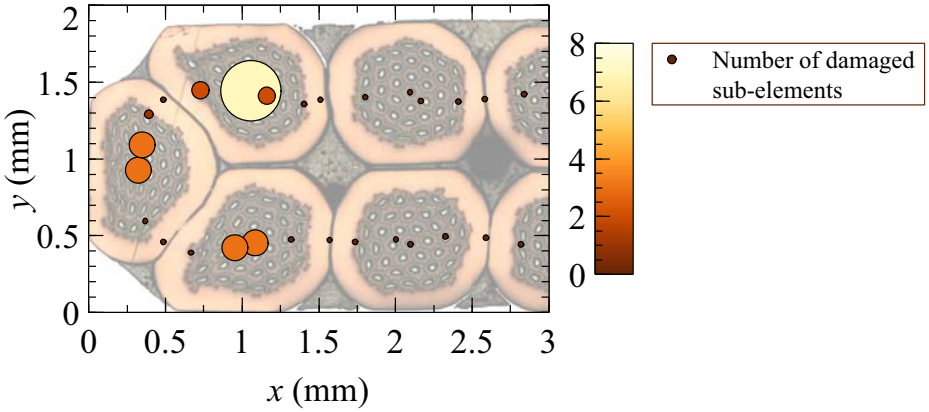

Figure 9: Number of damaged sub-elements identified per strand as a function of position in the cable cross-section, demonstrating that significant sub-element damage is present only at the cable edges. The plot is superimposed on an example of the cross-section (optical microscopy) in which the left-most three strands are close to the positions resulting in the greatest number of damaged sub-elements.

In distributed barrier wires with more regular sub-element geometry, damaged sub-elements have been reported to cluster radially along shear planes [10, 11]. In contrast, in the present wire, these

defects occur primarily in the outermost sub-elements as a result of their non-uniformity in the as-received wire. As this corresponds to some locations with lower strain states, this suggests that the number of damaged sub-elements could be reduced by optimisation of the sub-element geometry.

5.3. Superconducting Performance of Extracted Strands

Critical current measurements (Figure 10) reveal a very low I_c degradation (<1 % on average) on rolling and on cabling, considerably below the maximum 5 % specified. A modest reduction in RRR is observed (Table 3), but the values remain considerably higher than the specification level of 100.

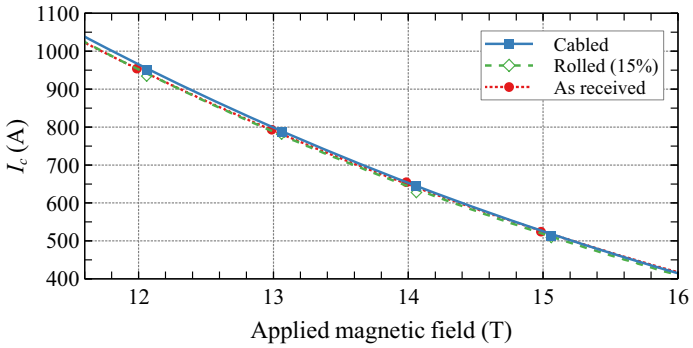

Figure 10: I_c of TVEL wire samples at 4.3 K in the as-received (round) condition, after rolling with 15 % reduction and extracted from the cable (from the same unit length)

Table 3. RRR of two selected TVEL wire samples in the as-received (round) condition, after rolling with 15 % reduction and extracted from the cable

Parameter	Piece length 1	Piece length 2
Round	228	271
Rolled (15 % reduction)	220	227
Extracted from cable	181	

It should be noted that an I_c measurement of an extracted strand samples multiple kink regions with high strand deformation, as the voltage tap separation is ~6 times the transposition pitch. This robustness of the I_c even in the presence of some damaged sub-elements is a common observation for distributed-barrier internal tin conductors, including those used for the HL-LHC Project.

It is often difficult to establish definitively from micrographs like those in Figure 8 if there are points of contact between the stabilising copper and the tin cores, but for a wire with irregular geometry it seems reasonable to assume that at least some localised tin leaks would occur. The high RRR provides no clear evidence of this; but the relatively short samples typically used for RRR measurement (including in the present study) are likely to sample no more than 1 kink region. A larger number of RRR measurements will therefore be assessed for cabling qualification.

6. Conclusions

The suitability for cabling of two internal tin Nb_3Sn wires produced for the FCC conductor development programme has been verified: a distributed barrier wire from TVEL and a common barrier distributed tin wire from JASTEC, both of which have a non-Cu J_c exceeding 1000 A/mm^2 at 16 T and 4.2 K. For both wires, the I_c and RRR of samples rolled with a reduction of 15 % meet the specification defined for HL-LHC. A 40-strand Rutherford cable has been produced from the TVEL wire, from which extracted strands meet the same I_c and RRR requirements.

Microscopy and image analysis have revealed details of the deformation behaviour, and identified aspects to consider in the further optimisation of both wire types. For the distributed barrier wire, sub-element damage in the most heavily deformed sites during cabling arises due to the irregular geometry of peripheral sub-elements. For distributed tin wire with a common barrier, a rolling reduction of 20 % gives rise to significant redistribution of tin and potential barrier breaches, and it is therefore possible they may occur locally during cabling. As deformation occurs primarily on planes through the copper matrix and tin cores, the overall behaviour is expected to depend on the availability of copper pathways between Nb sub-elements, and may be influenced by the interfacial bonding between modules during assembly. The non-uniformity of the diffusion barrier is a contributing factor, itself related to the alternating hardness of tin and filamentary regions around the wire periphery. It should be noted that both wires reported here are developmental deliverables of on-going R&D collaborations, and the next generation of improved conductors is already being produced.

Cabling trials are scheduled at CERN for distributed tin wire from JASTEC and KAT, and further characterisation of the TVEL trial cable is planned. In parallel, new trial wires are under development at TVEL and JASTEC. Considering the evidence of degradation that may occur for rolling reductions only slightly exceeding 15 %, analysis of this material will include rolling studies at 20 % reduction, and the evaluation of a larger number of adjacent RRR samples from extracted strands. Mechanical modelling is in progress to assist with optimising the suitability for cabling of future wire designs.

Acknowledgments

The authors would like to thank K. Bogdanowicz, A. T. Perez Fontenla and colleagues in CERN's Metallurgy and Metrology section (EN-MME-MM) for metallography and electron microscopy, and the technical staff of the Superconductors and Superconducting Devices section (TE-MSC-SCD) for their help with sample preparation, cabling, heat treatments and electrical measurements.

The support and collaboration of the wire suppliers for the present study, JASTEC and TVEL, KEK, and all participants in the FCC conductor development programme are gratefully acknowledged.

References

[1] Abada A *et al.* 2019 *Eur. Phys. J. C* **79** 474
Abada A *et al.* 2018 *CERN Accelerator Reports CERN-ACC-2018-0056. Future Circular Collider Study. Volume 1: Physics Opportunities. Conceptual Design Report*, ed Mangano M *et al.* (Geneva: CERN)

[2] Abada A *et al.* 2019 *Eur. Phys. J. Spec. Top.* **228** 755–1107
Abada A *et al.* 2018 *CERN Accelerator Reports CERN-ACC-2018-0058. Future Circular Collider Study. Volume 3: The Hadron Collider (FCC-hh). Conceptual Design Report*, ed Benedikt M *et al.* (Geneva: CERN)

[3] Ballarino A *et al.* 2019 *IEEE Trans. Appl. Supercond.* **29** 6000709

[4] Fleiter J, Peggiani S, Bonasia A and Ballarino A 2018 *IEEE Trans. Appl. Supercond.* **28** 4802205

[5] Oberli L 2013 *IEEE Trans. Appl. Supercond.* **23** 4800704

[6] Bordini B, Richter D, Alknes P, Ballarino A, Bottura L and Oberli L 2013 *IEEE Trans. Appl. Supercond.* **23** 7100806

[7] Hopkins S C, Baskys A, Canós Valero A and Ballarino A 2019 *IEEE Trans. Appl. Supercond.* **29** 6001307

[8] Pantsyrny V 2017 FCC Conductor Development in Russia *FCC Week 2017 (Berlin, Germany, May 2017)* https://indico.cern.ch/event/556692/contributions/2591623/

[9] Kawashima S, Kawarada T, Kato H, Murakami Y, Sugano M, Oguro H and Awaji S 2020 *IEEE Trans. Appl. Supercond.* **30** 6000105

[10] Barzi E and Zlobin A V 2016 *IEEE Trans. Nucl. Sci.* **63** 783–803

[11] Rochepault E, Arbelaez D, Pong I and Dietderich D R 2015 *IEEE Trans. Appl. Supercond.* **25** 8800905